



Photonic dephasing dynamics and the role of initial correlations

Sina Hamedani Raja ^{1,*}, K. P. Athulya,² Anil Shaji,² and Jyrki Piilo ¹

¹*QTF Centre of Excellence, Turku Centre for Quantum Physics, Department of Physics and Astronomy, University of Turku, FI-20014 Turun yliopisto, Finland*

²*School of Physics, Indian Institute of Science Education and Research, Thiruvananthapuram, Kerala 695551, India*



(Received 30 January 2020; accepted 30 March 2020; published 28 April 2020)

Photons are useful quantum systems for investigating the fundamental and practical aspects of dephasing, decoherence, and other types of open quantum dynamics. However, descriptions of open dynamics of photonic systems are usually in terms of decoherence functions and in many cases an explicit master-equation-based description is not available. This is particularly true when considering multipartite photonic open systems having possibly correlated environments. We obtain generic master equations for the reduced dephasing dynamics of a two-photon polarization state coupled to respective frequency degrees of freedom when the frequency degrees of freedom that form the environment are initially correlated. Our results show the explicit dependence of the operator form of the master equation and the decay rates on these correlations as well as on various types of frequency distributions. Furthermore, we use the recently developed *bath-positive decomposition* method to treat an initially correlated polarization-frequency state of a photon and demonstrate how this allows us to gain new insight and detailed information on how the contributions of different origins influence the photonic dephasing.

DOI: [10.1103/PhysRevA.101.042127](https://doi.org/10.1103/PhysRevA.101.042127)

I. INTRODUCTION

Understanding open-system dynamics and decoherence is important in several areas of quantum physics [1,2]. During the last 10 years, there have been significant developments in both understanding the role of non-Markovian memory-effects [3–7] and developing improved tools and techniques to treat open-system dynamics [8]. Here, one of the common themes is the role that various types of correlations play in open-system dynamics. In particular, understanding the initial correlations between composite environments [9–14] and the role of initial system-environment correlations [15–23] has led to fundamental insights as well as practical knowledge regarding open systems.

Photons provide a common and highly controllable system where the influence of correlations can be studied both conceptually and practically [9–14,22]. Here, the polarization state of the photon is the open system and its frequency is the environment. Polarization and frequency are coupled via birefringence, leading to dephasing of a polarization state of the photon(s). The control of the initial frequency distribution allows for the engineering of the decoherence and it is also possible to exploit various correlations for single-photon or composite two-photon systems [9,22,24].

On the one hand, dephasing dynamics of photons has often been described using the concept of decoherence functions and subsequent family of completely positive (CP) dynamical maps, in the past. On the other hand, master equations are one of the most common tools for treating open-system dynamics [1]. However, master equations have not been used extensively when considering multipartite photonic systems and

dephasing. We consider first a bipartite two-photon system where the initial system-environment state is factorized while there exist initial correlations between the environmental states. It has been shown earlier that this induces nonlocal memory effects in open-system dynamics [9,10]. However, the role of these types of initial correlations and nonlocal memory effects has not been considered on the level of master equations before, to the best of our knowledge. We derive generic master equations which display explicitly the role of initial correlations both on the dephasing rates and on the operator form of the master equation. This allows us also to reveal how even quite straightforward changes in the initial environmental state drastically change the description of photonic dephasing and increase the number of jump operators in the master equation.

Continuing within the framework of correlations and open systems, we also study another long-standing problem in this context. This is the role that initial system-environment correlations play in open-system dynamics. Here, our interest is to see what kind of insight the recently developed *bath-positive decomposition* method [21] allows when studying the open dynamics of the polarization states. This very general method is based on decomposing an initial arbitrary system-environment state to a number of terms where each term can be treated with its individual CP map. We show that for single-photon dephasing, this decomposition allows the description, in an insightful way, of how initial correlations influence the dynamics beyond the contribution arising from the factorized part.

The structure of the paper is the following. In the next section (Sec. II) we describe briefly the basics of photonic dephasing. In Sec. III we focus on the correlations within the composite environment, derive various master equations in this context, and discuss the insight they provide.

*sihara@utu.fi

Section IV, in turn, describes the initially correlated system-environment case for single photons and Sec. V concludes the paper.

II. PRELIMINARIES WITH SINGLE-PHOTON DEPHASING DYNAMICS

We start with a brief recall of the single-photon dephasing model [24]. The polarization degree of freedom and frequency degree of freedom of a photon correspond to the open system and its environment, respectively. To begin, we consider the initially factorized joint polarization-frequency state

$$\hat{\rho}_{SE}(0) = \hat{\rho}_S(0) \otimes |\Omega\rangle\langle\Omega|. \quad (1)$$

Here, $\hat{\rho}_S(0)$ is the density operator of the initial polarization state and

$$|\Omega\rangle = \int d\omega g(\omega)|\omega\rangle \quad (2)$$

is the initial frequency state, where $g(\omega)$ is the probability amplitude that the photon has frequency ω . The polarization Hilbert space is discrete and spanned by the horizontal-vertical polarization basis $\{|h\rangle, |v\rangle\}$, while the Hilbert space of the frequency degree of freedom is spanned by the continuous frequency basis $\{|\omega\rangle\}$.

The system-environment—or polarization-frequency—interaction is provided by the Hamiltonian ($\hbar = 1$)

$$\hat{H} = (n_h|h\rangle\langle h| + n_v|v\rangle\langle v|) \otimes \int d\omega \omega |\omega\rangle\langle\omega|, \quad (3)$$

where n_h (n_v) is the refraction index for polarization component h (v). For interaction time t , and tracing over the frequency, the reduced polarization state is

$$\hat{\rho}_S(t) = \begin{pmatrix} \langle h|\rho_S(0)|h\rangle & \kappa(t)\langle h|\rho_S(0)|v\rangle \\ \kappa(t)^*\langle v|\rho_S(0)|h\rangle & \langle v|\rho_S(0)|v\rangle \end{pmatrix}. \quad (4)$$

Here, the dephasing dynamics is given by the decoherence function

$$\kappa(t) = \int d\omega |g(\omega)|^2 e^{-i\Delta n\omega t}, \quad (5)$$

where $\Delta n \equiv n_v - n_h$. Note that $0 \leq |\kappa(t)| \leq 1$ for all times $t \geq 0$ and $|\kappa(0)| = 1$.

Equation (4) describes a t -parametrized CP map $\hat{\Phi}_t$, such that $\hat{\rho}_S(t) = \hat{\Phi}_t[\hat{\rho}_S(0)]$, and its corresponding master equation takes the form

$$\frac{d}{dt}\hat{\rho}_S(t) = -i\frac{\nu(t)}{2}[\hat{\sigma}_z, \hat{\rho}_S(t)] + \frac{\gamma(t)}{2}[\hat{\sigma}_z\hat{\rho}_S(t)\hat{\sigma}_z - \hat{\rho}_S(t)]. \quad (6)$$

Here, $\hat{\sigma}_z$ is the Pauli z operator and the rates $\nu(t)$ and $\gamma(t)$ can be expressed in terms of the decoherence function $\kappa(t)$ as

$$\gamma(t) = -\text{Re}\left[\frac{1}{\kappa(t)}\frac{d\kappa(t)}{dt}\right], \quad \nu(t) = -\text{Im}\left[\frac{1}{\kappa(t)}\frac{d\kappa(t)}{dt}\right], \quad (7)$$

where, $\text{Re}[\cdot]$ and $\text{Im}[\cdot]$ indicate the real and imaginary parts, respectively.

Equation (7) shows that once the decoherence function $\kappa(t)$ is obtained from Eq. (5), then we can derive the corresponding rates in master equation (6). Indeed, the decoherence function $\kappa(t)$ in Eq. (5) is the Fourier transformation of the initial frequency probability distribution $P(\omega) = |g(\omega)|^2$, and therefore the control of this distribution allows us to study various types of dephasing maps and to engineer the form and time dependence of the dephasing rate $\gamma(t)$ in master equation (6).

For example, a Gaussian frequency distribution with variance σ^2 and mean value $\bar{\omega}$, i.e.,

$$P(\omega) = \frac{\exp[-(\omega - \bar{\omega})^2/2\sigma^2]}{\sqrt{2\pi}\sigma},$$

leads to a positive and time-dependent dephasing rate $\gamma(t) = \Delta n^2\sigma^2 t$, which presents a time-dependent Markovian dynamics. On the other hand, a Lorentzian distribution

$$P(\omega) = \frac{\lambda}{\pi[(\omega - \omega_0)^2 + \lambda^2]}$$

results in a constant decay rate $\gamma = \lambda\Delta n$, corresponding to dynamical semigroup and Lindblad-Gorini-Kossakowski-Sudarshan (LGKS) dynamics [25,26]. We note that the latter case has also been reported in [27] and [28]. The transition from a Markovian to a non-Markovian regime, in turn, is observed with further modifications of the frequency distribution [24].

In the following, we generalize the master equation, Eq. (6), to the two-photon case. In particular, we are interested in how the initial correlations between the frequencies of the two photons influence the various dephasing rates and the operator form of the corresponding master equation for a bipartite open system.

III. MASTER EQUATION FOR TWO-PHOTON DEPHASING DYNAMICS: ROLE OF THE INITIALLY CORRELATED JOINT FREQUENCY DISTRIBUTION

Consider a pair of photons, labeled a and b , whose total polarization-frequency initial state is again in a factorized form,

$$\hat{\rho}_{SE}(0) = \hat{\rho}_S(0) \otimes |\Omega\rangle\langle\Omega|, \quad (8)$$

where now

$$|\Omega\rangle = \int d\omega_a \int d\omega_b g(\omega_a, \omega_b)|\omega_a, \omega_b\rangle \quad (9)$$

is the initial state of the two-photon frequency degree of freedom and the corresponding joint probability distribution is $P(\omega_a, \omega_b) = |g(\omega_a, \omega_b)|^2$. The initial polarization state is $\hat{\rho}_S(0)$, whose Hilbert space is spanned by the bipartite basis $\{|hh\rangle, |hv\rangle, |vh\rangle, |vv\rangle\}$.

The polarization of each photon interacts locally with its own frequency and therefore the system-environment interaction Hamiltonian for the two photons is the sum of the two local contributions [9]:

$$\hat{H} = \hat{H}_a \otimes \hat{I}_b + \hat{I}_a \otimes \hat{H}_b. \quad (10)$$

Here, each local term is given by Eq. (3) and \hat{I}_a (\hat{I}_b) is the identity operator for photon a (photon b).

We write the initial bipartite polarization state $\hat{\rho}_S(0)$ as

$$\hat{\rho}_S(0) = \sum_{\alpha, \beta} \sum_{\alpha', \beta'} p_{\alpha\beta, \alpha'\beta'} |\alpha\beta\rangle \langle \alpha'\beta'|,$$

$$\hat{\rho}_S(t) = \begin{pmatrix} P_{hh, hh} & \kappa_b(t) P_{hh, hv} & \kappa_a(t) P_{hh, vh} & \kappa_{ab}(t) P_{hh, vv} \\ \kappa_b^*(t) P_{hv, hh} & P_{hv, hv} & \Lambda_{ab}(t) P_{hv, vh} & \kappa_a(t) P_{hv, vv} \\ \kappa_a^*(t) P_{vh, hh} & \Lambda_{ab}^*(t) P_{vh, hv} & P_{vh, vh} & \kappa_b(t) P_{vh, vv} \\ \kappa_{ab}^*(t) P_{vv, hh} & \kappa_a^*(t) P_{vv, hv} & \kappa_b(t)^* P_{vv, vh} & P_{vv, vv} \end{pmatrix}. \quad (11)$$

Here, the local decoherence functions for photon $j = a, b$ are given by

$$\kappa_j(t) = \int d\omega_a \int d\omega_b |g(\omega_a, \omega_b)|^2 e^{-i\Delta n \omega_j t}, \quad (12)$$

and the nonlocal ones by

$$\kappa_{ab}(t) = \int d\omega_a \int d\omega_b |g(\omega_a, \omega_b)|^2 e^{-i\Delta n(\omega_a + \omega_b)t}, \quad (13)$$

and

$$\Lambda_{ab}(t) = \int d\omega_a \int d\omega_b |g(\omega_a, \omega_b)|^2 e^{-i\Delta n(\omega_a - \omega_b)t}. \quad (14)$$

The density matrix evolution given by Eqs. (11)–(14) can also be described by a t -parametrized CP dynamical map $\hat{\Phi}_t$, such that

$$\hat{\rho}_S(t) = \hat{\Phi}_t[\hat{\rho}_S(0)]. \quad (15)$$

It is important to note that when the initial joint frequency distribution factorizes, $P(\omega_a, \omega_b) = P_a(\omega_a) \times P_b(\omega_b)$, then the global decoherence functions are products of the local ones, i.e., $\kappa_{ab}(t) = \kappa_a(t)\kappa_b(t)$ and $\Lambda_{ab}(t) = \kappa_a(t)\kappa_b^*(t)$. Subsequently, the map for the bipartite photon system is the tensor product of the local CP maps $\hat{\Phi}_t = \hat{\Phi}_t^{(a)} \otimes \hat{\Phi}_t^{(b)}$. However, when the initial frequency distribution does not factorize, $P(\omega_a, \omega_b) \neq P_a(\omega_a) \times P_b(\omega_b)$, and contains correlations, then the map for the bipartite system is no longer the product of the local maps, $\hat{\Phi}_t \neq \hat{\Phi}_t^{(a)} \otimes \hat{\Phi}_t^{(b)}$ [9]. Now, we are interested in how to derive the generator of the corresponding nonlocal bipartite dynamical map and what the modifications in the corresponding dephasing master equations are when the amount of initial frequency correlations changes.

We begin our derivation by writing the dynamical map formally as

$$\hat{\Phi}_t = \exp \left[\int_0^t d\tau \hat{\mathcal{L}}_\tau \right], \quad (16)$$

where $\hat{\mathcal{L}}_t$ is the generator of the dynamics. Finding an expression for the generator then provides us the master equation we want to construct as

$$\frac{d}{dt} \hat{\rho}_S(t) = \hat{\mathcal{L}}_t[\hat{\rho}_S(t)]. \quad (17)$$

Provided that the map in Eq. (16) is invertible and its derivative is well defined, one can obtain the generator as

$$\hat{\mathcal{L}}_t = \frac{d}{dt} \hat{\Phi}_t \circ \hat{\Phi}_t^{-1}. \quad (18)$$

To find the generator in Eq. (18) we need a suitable representation for the dynamical map $\hat{\Phi}_t$. With this in mind, we

with sums over h and v . After interaction time t , the polarization state is [9]

expand the two-photon density matrix $\hat{\rho}_S(t)$ in terms of a complete and orthonormal operator basis $\{\hat{F}_\alpha\}$. Specifically, we choose here 15 generators of SU(4), whose exact expressions can be found in [29], plus $\hat{F}_1 = \hat{I}/\sqrt{4}$, such that $\text{Tr}[\hat{F}_i^\dagger \hat{F}_j] = \delta_{ij}$. It is noteworthy that one can alternatively use the basis constructed by the tensor product of Pauli matrices plus the identity. Fixing the basis for the representation, the two-photon polarization state at time t is

$$\hat{\rho}_S(t) = \sum_{\alpha=1}^{16} r_\alpha(t) \hat{F}_\alpha, \quad r_\alpha(t) = \text{Tr}[\hat{F}_\alpha \hat{\rho}_S(t)], \quad (19)$$

where coefficients $\{r_\alpha\}$ form the generalized Bloch vector corresponding to the state $\hat{\rho}_S(t)$ as

$$\vec{r}(t) = (1/2, r_2(t), \dots, r_{16}(t))^T. \quad (20)$$

By using Eq. (19) for both $\hat{\rho}_S(t)$ and $\hat{\rho}_S(0)$, we can write Eq. (15) as

$$r_\alpha(t) = \sum_{\beta} [\hat{\Phi}_t]_{\alpha\beta} r_\beta(0), \quad (21)$$

where $[\hat{\Phi}_t]$ is the transformation matrix corresponding to the map $\hat{\Phi}_t$ represented in the basis $\{\hat{F}_\alpha\}$. Elements of this matrix depend on the decoherence functions given in Eqs. (12)–(14) and each column can be systematically calculated by using a proper pair of initial and evolved states [cf. Eq. (11)]. One can proceed to find the matrix representation of the generator by calculating the derivative and inverse of $[\hat{\Phi}_t]$ and using them in Eq. (18), such that

$$[\hat{\mathcal{L}}_t] = \frac{d}{dt} [\hat{\Phi}_t][\hat{\Phi}_t]^{-1}, \quad (22)$$

where we have replaced operator multiplication with matrix multiplication.

Let us now consider the generator in a Lindblad operator form,

$$\hat{\mathcal{L}}_t[\hat{\rho}_S(t)] = -i[\hat{H}(t), \hat{\rho}_S(t)] + \sum_{\alpha=2}^{16} \sum_{\beta=2}^{16} R_{\alpha\beta}(t) \times \left(\hat{F}_\alpha \hat{\rho}_S(t) \hat{F}_\beta^\dagger - \frac{1}{2} \{ \hat{F}_\beta^\dagger \hat{F}_\alpha, \hat{\rho}_S(t) \} \right),$$

where

$$\hat{H}(t) = \frac{-1}{2i} \sum_{\alpha=2}^{16} [R_{\alpha 1}(t) \hat{F}_\alpha - R_{1\alpha}(t)^* \hat{F}_\alpha^\dagger] \quad (23)$$

captures the environment-induced coherent dynamics and $R_{\alpha\beta}(t)$ with $\alpha, \beta = 2, 3, \dots, 16$ are elements of a 15×15

matrix providing the decay rates. Each element in the matrix representation of the generator then reads

$$[\hat{\mathcal{L}}_t]_{\alpha\beta} = \text{Tr}[\hat{F}_\alpha^\dagger \hat{\mathcal{L}}_t[\hat{F}_\beta]]. \quad (24)$$

Here we use Eq. (23) on the right-hand side. Finally, by elementwise comparison of Eq. (24) with Eq. (22) we find the decay rates of the Lindblad master equation, Eq. (23), in terms of the decoherence functions in Eqs. (12)–(14). Before proceeding further, let us note that the generator of a CP-divisible map always has a Lindblad form [2,25,26,29]. A map $\hat{\Phi}_t$ is CP divisible if it can be decomposed as $\hat{\Phi}_t = \hat{\Phi}_{t,s} \hat{\Phi}_s$, where the intermediate map $\hat{\Phi}_{t,s}$ is also a legitimate CP map for all $t \geq s \geq 0$ [30]. In this paper, however, we do not restrict ourselves to CP-divisible maps, and as we show later we also take non-Markovian dynamics into account.

After finding the general expression for the decay rate matrix, it turns out that it is quite sparse and can be reduced to a 3×3 matrix, which we denote $R(t)$. The corresponding subspace is spanned by only three generators of SU(4), which are linearly dependent on the operators $\hat{I}_2 \otimes \hat{\sigma}_z$, $\hat{\sigma}_z \otimes \hat{I}_2$, and $\hat{\sigma}_z \otimes \hat{\sigma}_z$. This is indeed intuitive because population elements of the density matrix are invariant upon a dephasing channel, so those terms that couple the levels must be absent. The explicit expression for the matrix $R(t)$, corresponding to a general frequency distribution, is provided in the Appendix. Considering this general result, we diagonalize it to rewrite the second term on the right-hand side of Eq. (23) in the form

$$\hat{\mathcal{D}}[\hat{\rho}_S(t)] = \sum_{\alpha=1}^3 \gamma_\alpha(t) \left[\hat{J}_\alpha \hat{\rho}_S(t) \hat{J}_\alpha^\dagger - \frac{1}{2} \{ \hat{J}_\alpha^\dagger \hat{J}_\alpha, \hat{\rho}_S(t) \} \right], \quad (25)$$

where

$$\begin{pmatrix} \gamma_1(t) & 0 & 0 \\ 0 & \gamma_2(t) & 0 \\ 0 & 0 & \gamma_3(t) \end{pmatrix} = UR(t)U^\dagger, \quad \hat{J}_\alpha = \sum_j U_{\alpha j} \hat{F}_j, \quad (26)$$

and U is the orthogonal transformation which diagonalizes the matrix $R(t)$. It is worth stressing that if the dynamical map in hand is CP divisible, then all decay rates will be nonnegative, i.e., $\gamma_i(t) \geq 0$ for all interaction times $t \geq 0$.

The above general results hold for arbitrary initial frequency distributions. In the following, we discuss explicitly initially correlated joint frequency distributions for the bivariate single- and double-peak Gaussian cases. These choices are motivated by their use in recent theoretical and experimental works (see, e.g., [9,14,24]) and their ability to account for the explicit influence of frequency correlations in the dephasing dynamics.

A. Single-peak bivariate Gaussian distribution

Consider the joint bivariate Gaussian frequency distribution $P_{ab}(\omega_a, \omega_b)$ and its covariance matrix C , such that $C_{ij} = \langle \omega_i \omega_j \rangle - \langle \omega_i \rangle \langle \omega_j \rangle$ for $i, j = a, b$ [9]. The correlation coefficient is now given by $K = C_{ab} / \sqrt{C_{aa} C_{bb}}$, such that $-1 \leq K \leq 1$. A fully anticorrelated initial frequency distribution has $K = -1$, which dictates that for any pair of ω_a and ω_b we have $\omega_a + \omega_b \equiv \omega_0$, with some constant frequency ω_0 . The means of the local single-photon frequency distributions are given by $(\bar{\omega}_a, \bar{\omega}_b)^T$ and we denote the difference between the local

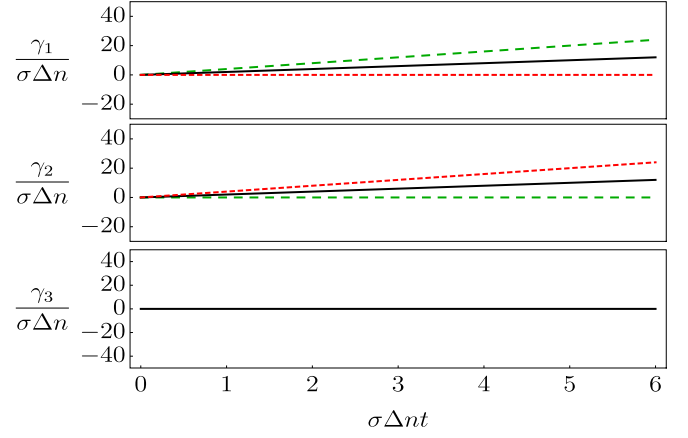


FIG. 1. Decay rates as a function of the normalized interaction time in the case of a single-peak Gaussian frequency distribution. Long-dashed green line, $K = -1$; solid black line, $K = 0$; and short-dashed red line, $K = 1$. Here we set $\Delta\omega/\sigma = 2$.

means $\bar{\omega}_a - \bar{\omega}_b = \Delta\omega$ and their sum $\bar{\omega}_a + \bar{\omega}_b = \omega_0$. Using Eqs. (12)–(14) and denoting the variance of the distribution σ^2 , the decoherence functions become

$$\kappa_a(t) = \exp\left[\frac{-\sigma^2 \Delta n^2 t^2 - i \Delta n t (\omega_0 + \Delta\omega)}{2}\right], \quad (27)$$

$$\kappa_b(t) = \exp\left[\frac{-\sigma^2 \Delta n^2 t^2 - i \Delta n t (\omega_0 - \Delta\omega)}{2}\right], \quad (28)$$

$$\kappa_{ab}(t) = \exp[-\sigma^2 \Delta n^2 t^2 (1 + K) - i \Delta n t \omega_0], \quad (29)$$

$$\Lambda_{ab}(t) = \exp[-\sigma^2 \Delta n^2 t^2 (1 - K) - i \Delta n t \Delta\omega]. \quad (30)$$

It is straightforward to check that the corresponding transformation matrix $[\Phi_t]$ for the generalized Bloch vector is always invertible when the time t is finite. After inserting the above expressions for the decay rate matrix $R(t)$ (see the Appendix), followed by diagonalization, we obtain the rates appearing in the master equation, (25), as

$$\gamma_1(t) = 2(1 - K)\sigma^2 \Delta n^2 t, \quad (31)$$

$$\gamma_2(t) = 2(1 + K)\sigma^2 \Delta n^2 t, \quad (32)$$

$$\gamma_3(t) = 0 \quad (33)$$

and the corresponding jump operators

$$\hat{J}_1 = \frac{1}{2\sqrt{2}}(\hat{I}_2 \otimes \hat{\sigma}_z + \hat{\sigma}_z \otimes \hat{I}_2), \quad (34)$$

$$\hat{J}_2 = \frac{1}{2\sqrt{2}}(\hat{I}_2 \otimes \hat{\sigma}_z - \hat{\sigma}_z \otimes \hat{I}_2), \quad (35)$$

$$\hat{J}_3 = \frac{1}{2}\hat{\sigma}_z \otimes \hat{\sigma}_z. \quad (36)$$

Dephasing rates γ_1 and γ_2 are linear functions of time and their slopes depend on the correlation coefficient K . Figure 1 displays the rates for $K = -1, 0, 1$. Since all the rates are nonnegative and the first two are time dependent, this leads to CP-divisible dynamics, which, however, does not fulfill the LGKS semigroup property. It is also interesting to note here the absence of the jump operator $\hat{\sigma}_z \otimes \hat{\sigma}_z$ since the

corresponding rate γ_3 is always equal to 0. Moreover, the role of the environmental correlation coefficient K of the initial joint frequency distribution is now explicit in expressions (31)–(33). When $K = 1$ ($K = -1$) the rate $\gamma_1 = 0$ ($\gamma_2 = 0$) and we are left with only one dephasing channel, given by \hat{J}_2 (\hat{J}_1). When there are no initial correlations between the two environments, $K = 0$, then $\gamma_1(t) = \gamma_2(t)$. Subsequently, the corresponding generator and master equation contain equally weighted contributions of the two local jump operators \hat{J}_1 and \hat{J}_2 . Changing the value of the initial correlations K allows us then to tune the dynamics between the above-mentioned extreme cases.

It is also worth discussing similarities and differences between our photonic model and the two-qubit model interacting with a common environment [31–34]. In the latter model two qubits are spatially separated by a distance D , while they both interact with the same physical and common bosonic environment. It is interesting that the master equation describing this model has the exact same operator form and jump operators [34] obtained in Eqs. (34) to (36). In addition, the decay rates derived in [34] exhibit a similar dependence on the distance D , as our decay rates here depend on the correlation coefficient K . Moreover, when $D \rightarrow \infty$, the dynamical map will be factorized to $\hat{\Phi}_t = \hat{\Phi}_t^{(a)} \otimes \hat{\Phi}_t^{(b)}$, with the superscripts corresponding to each qubit. The same behavior is also captured here when $K \rightarrow 0$. However, it is worth keeping in mind that in our case the two environments are distinct physical entities and the tuning of the generator—or form of the master equation—is obtained by changing the initial bipartite environmental state. Furthermore, we can tune the generator continuously between the fully correlated and the anticorrelated cases.

B. Double-peak bivariate Gaussian distribution

We consider a double-peak frequency distribution as the sum of two single-peak bivariate Gaussian distributions, already used in [14], such that

$$P(\omega_a, \omega_b) = [P_1(\omega_a, \omega_b) + P_2(\omega_a, \omega_b)]/2. \quad (37)$$

We assume that both single-peak terms have the same correlation coefficient K and standard deviation σ , but their means are located at $(\omega_0/2 - \Delta\omega/2, \omega_0/2 + \Delta\omega/2)^T$ and $(\omega_0/2 + \Delta\omega/2, \omega_0/2 - \Delta\omega/2)^T$, respectively. Please note that the correlation coefficient K of each single-peak distribution P_1 (P_2) does not equal the actual correlation coefficient of the bivariate distribution P , obtained by its covariance matrix. In more detail, whenever we have nonzero K for each single peak, we have a nonzero correlation in P . But note that if $K = 0$, then we still have a correlation in P as long as we have nonzero peak separation, $\Delta\omega \neq 0$.

The decoherence functions calculated from Eqs. (12)–(14) become

$$\kappa_a(t) = \exp\left[\frac{-\sigma^2 \Delta n^2 t^2 - it \Delta n \omega_0}{2}\right] \cos\left(\frac{t \Delta n \Delta \omega}{2}\right), \quad (38)$$

$$\kappa_b(t) = \kappa_a(t), \quad (39)$$

$$\kappa_{ab}(t) = \exp[-\sigma^2 \Delta n^2 t^2 (1 + K) - it \Delta n \omega_0], \quad (40)$$

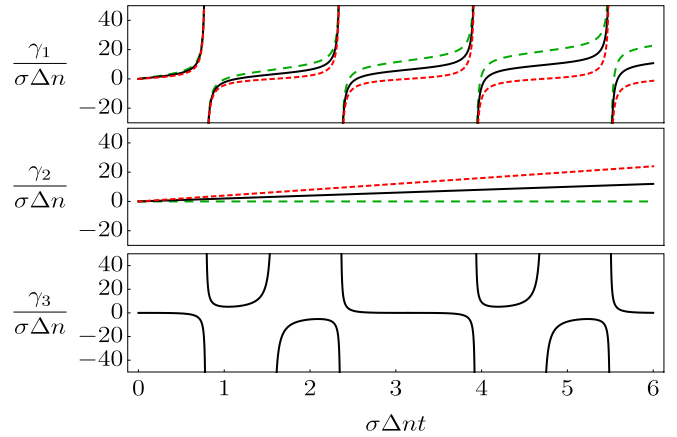


FIG. 2. Decay rates as a function of the normalized interaction time in the case of a double-peak Gaussian frequency distribution. Long-dashed green line, $K = -1$; solid black line, $K = 0$; and short-dashed red line, $K = 1$. Here we set $\Delta\omega/\sigma = 2$.

$$\Lambda_{ab}(t) = \exp[-\sigma^2 \Delta n^2 t^2 (1 - K)] \cos(t \Delta n \Delta \omega). \quad (41)$$

By using the general results obtained earlier, in a similar manner compared to the single-peak case, we obtain the dephasing rates

$$\gamma_1(t) = 2(1 - K)\sigma^2 \Delta n^2 t + \tan(t \Delta n \Delta \omega) \Delta n \Delta \omega, \quad (42)$$

$$\gamma_2(t) = 2(1 + K)\sigma^2 \Delta n^2 t, \quad (43)$$

$$\gamma_3(t) = \frac{1}{2} \tan\left(\frac{t \Delta n \Delta \omega}{2}\right) [1 - \sec(t \Delta n \Delta \omega)] \Delta n \Delta \omega. \quad (44)$$

The corresponding jump operators $\{\hat{J}_1, \hat{J}_2, \hat{J}_3\}$ are the same as in the single-peak case; see Eqs. (34)–(36). In the limit $\Delta\omega \rightarrow 0$ corresponding to the single-peak case, the rates, (42)–(44), reduce to those given by Eqs. (31)–(33).

Figure 2 displays the rates for $K = -1, 0$, and 1 . The dephasing rate γ_2 remains the same as in the single-peak case. However, the rate γ_1 —corresponding to \hat{J}_1 including the sum of the local jump operators—changes. The rate now includes an extra term, coming from the peak separation $\Delta\omega$, and an oscillatory part displaying negative values of the rate as a function of the time. This also leads to non-Markovian dephasing dynamics which is not CP divisible. It is even more striking that introducing the double-peak frequency structure now opens an additional dephasing channel since the rate γ_3 is nonzero. Here, the corresponding jump operator $\hat{J}_3 = \frac{1}{2} \hat{\sigma}_z \otimes \hat{\sigma}_z$ displays a joint bipartite structure, in contrast to local features of \hat{J}_1 and \hat{J}_2 . This is an interesting observation since the system-environment interaction Hamiltonian is the same as before, having only local interactions [see Eq. (10)], while the only change introduced is going from a single- to a double-peak structure of the initial bipartite environmental state. It is also noteworthy that even though γ_3 is independent of K , its functional form is nontrivial since it contains the peak separation $\Delta\omega$ and trigonometric functions.

There is a somewhat subtle mathematical point related to the behavior of rates γ_1 [Eq. (42)] and γ_3 [Eq. (44)] which needs attention. Indeed, $\gamma_1(t)$ and $\gamma_3(t)$ diverge at isolated

points in time. Subsequently, the corresponding dynamical maps are noninvertible at these points. According to Eq. (21), the generalized Bloch vector of the two-photon polarization state at time t reads

$$\vec{r}(t) = \begin{pmatrix} \frac{1}{2} \\ \Gamma_0 \cos(t \Delta \Omega / 2) [\cos(t \Omega_0 / 2) r_2 - \sin(t \Omega_0 / 2) r_3] \\ \Gamma_0 \cos(t \Delta \Omega / 2) [\cos(t \Omega_0 / 2) r_3 + \sin(t \Omega_0 / 2) r_2] \\ r_4 \\ \Gamma_0 \cos(t \Delta \Omega / 2) [\cos(t \Omega_0 / 2) r_5 - \sin(t \Omega_0 / 2) r_6] \\ \Gamma_0 \cos(t \Delta \Omega / 2) [\cos(t \Omega_0 / 2) r_6 + \sin(t \Omega_0 / 2) r_5] \\ \Gamma_- \cos(t \Delta \Omega) r_7 \\ \Gamma_- \cos(t \Delta \Omega) r_8 \\ r_9 \\ \Gamma_+ [\cos(t \Omega_0) r_{10} - \sin(t \Omega_0) r_{11}] \\ \Gamma_+ [\cos(t \Omega_0) r_{11} + \sin(t \Omega_0) r_{10}] \\ \Gamma_0 \cos(t \Delta \Omega / 2) [\cos(t \Omega_0 / 2) r_{12} - \sin(t \Omega_0 / 2) r_{13}] \\ \Gamma_0 \cos(t \Delta \Omega / 2) [\cos(t \Omega_0 / 2) r_{13} + \sin(t \Omega_0 / 2) r_{12}] \\ \Gamma_0 \cos(t \Delta \Omega / 2) [\cos(t \Omega_0 / 2) r_{14} - \sin(t \Omega_0 / 2) r_{15}] \\ \Gamma_0 \cos(t \Delta \Omega / 2) [\cos(t \Omega_0 / 2) r_{15} + \sin(t \Omega_0 / 2) r_{14}] \\ r_{16} \end{pmatrix}, \quad (45)$$

where we have defined $\Gamma_0 = \exp[-\sigma^2 \Delta n^2 t^2 / 2]$, $\Gamma_{\pm} = \exp[-\sigma^2 \Delta n^2 t^2 (1 \pm K)]$, $\Delta \Omega = \Delta n \Delta \omega$, $\Omega_0 = \Delta n \omega_0$, and $\vec{r}(0) = (1/2, r_2, r_3, \dots, r_{16})^T$ is the initial Bloch vector. One can check that all of the different initial vectors (states) that share the same values of $r_4, r_7, r_8, r_9, r_{10}, r_{11}$, and r_{16} are mapped to the same vector (state) at $t = \pi / \Delta \Omega$. This many-to-one nature of the map—at these isolated times—makes it noninvertible. Although all the trajectories corresponding to the aforementioned initial vectors end up together at the isolated points, it is evident that they continue their different paths immediately after this. This can be seen in the following way. Consider the generator of the master equation in matrix form and its action on the generalized Bloch vector. We see that while some rates diverge at certain points in time, it is precisely at these points that the generalized Bloch vector components—with which the rates get multiplied—all go to 0. In more detail, we have

$$\frac{d}{dt} r_{\alpha}(t) = \sum_{\beta} [\hat{\mathcal{L}}_t]_{\alpha\beta} r_{\beta}(t), \quad (46)$$

therefore, the product of the divergent rate with the zero-value component leads to a finite rate of change of the Bloch vector which allows us to continue propagation of each state forward in time. Accordingly, following the trajectories immediately before they unite at a single point lets us identify each of them immediately after this, when they separate again. We see therefore that in spite of the divergences in the rates, the master equation we have obtained describes the dephasing evolution of the two-photon polarization state in a meaningful way. It is also noteworthy that the divergent decoherence rates in master equations have appeared in earlier literature many times, e.g., in the prominent resonant Jaynes-Cummings model [1].

IV. SINGLE-PHOTON DEPHASING WITH INITIAL POLARIZATION-FREQUENCY CORRELATIONS

We have described above how initial correlations between the composite environmental states influence the generator of the dynamical map and the corresponding master equation for photonic dephasing. In this section we continue with initial correlations but take a different perspective by considering a nonfactorized initial system-environment state for a single qubit. This is motivated by the recent observation that initial system-environment correlations can be exploited for arbitrary control of single-qubit dephasing [22]. We revisit this problem and obtain insight by exploiting the very recently developed general method of *bath-positive decomposition* (B+ decomposition) [21]. In general, the presence of initial system-environment correlations implies that the open-system evolution is not described by a CP dynamical map [15–20]. However, the B+ decomposition method allows us to treat this case with a set of CP maps, where each term of the decomposition is evolved over time with its individual CP map [21].

A. Preliminaries on B+ decomposition for an initially correlated system-environment state

Following [21] we begin by considering an arbitrary system-environment state—in the corresponding Hilbert space $\mathcal{H} = \mathcal{H}_S \otimes \mathcal{H}_E$ —and write it as

$$\hat{\rho}_{SE}(0) = \sum_{\alpha} w_{\alpha} \hat{Q}_{\alpha} \otimes \hat{\rho}_{\alpha}. \quad (47)$$

Here, $\{\hat{Q}_{\alpha}\}$ forms a basis (possibly overcomplete) for operators on \mathcal{H}_S , and $\{\hat{\rho}_{\alpha}\}$ are valid environmental density operators on \mathcal{H}_E . Note that \hat{Q}_{α} need not be positive or trace orthogonal, so they may not constitute proper density matrices in the system Hilbert space. However, when the initial state is factorized, this summation reduces to a single term, $\hat{\rho}_{SE}(0) = \hat{\rho}_S(0) \otimes \hat{\rho}_E(0)$, corresponding to reduced states of the open system and environment, respectively. In general, the number of terms in this summation is restricted by $1 \leq N \leq d^2$, where d is the dimension of the system Hilbert space [21]. All the information about the initial state of the open system is incorporated in the weights w_{α} , such that $\hat{\rho}_S(0) = \text{Tr}_E[\hat{\rho}_{SE}(0)] = \sum w_{\alpha} \hat{Q}_{\alpha}$. Although \hat{Q}_{α} may not be legitimate density operators for the open system, those expressed by $\hat{\rho}_{\alpha}$ are valid density operators for the environment. This means that the factorized form of the terms in (47) allows us to treat the dynamics of the open-system state as the weighted sum of legitimate CP maps acting on \hat{Q}_{α} . In more detail, if the total system-environment evolves due to a unitary operator $\hat{U}(t)$, one has

$$\begin{aligned} \hat{\rho}_S(t) &= \sum_{\alpha} w_{\alpha} \text{Tr}_E[\hat{U}(t)(\hat{Q}_{\alpha} \otimes \hat{\rho}_{\alpha})\hat{U}(t)^{\dagger}] \\ &= \sum_{\alpha} w_{\alpha} \hat{\Phi}_t^{(\alpha)}[\hat{Q}_{\alpha}], \end{aligned} \quad (48)$$

where

$$\hat{\Phi}_t^{(\alpha)}[\cdot] := \text{Tr}_E[\hat{U}(t)(\cdot \otimes \hat{\rho}_{\alpha})\hat{U}(t)^{\dagger}]. \quad (49)$$

Since all maps of the form given in Eq. (49) are CP, all previous tools for studying CP maps are applicable here. In particular, one can investigate the properties of each CP map $\Phi_i^{(\alpha)}$ and see how they are connected to the presence of initial correlations.

For example, consider single-qubit dynamics in the presence of initial system-environment correlations [21]. Using completeness of the Pauli sigma basis $\{\hat{I}_2, \hat{\sigma}_x, \hat{\sigma}_y, \hat{\sigma}_z\}$, we have

$$\hat{\rho}_{\text{SE}}(0) = \sum_{\alpha=0,x,y,z} w_\alpha \hat{Q}_\alpha \otimes \hat{\rho}_\alpha, \quad (50)$$

in which

$$\hat{Q}_0 = \frac{1}{2}(\hat{I}_2 - \hat{\sigma}_x - \hat{\sigma}_y - \hat{\sigma}_z), \quad (51)$$

$$\hat{Q}_\alpha = \frac{1}{2}\hat{\sigma}_\alpha \quad \text{for } \alpha = x, y, z \quad (52)$$

and

$$\hat{\rho}_0 = \text{Tr}_S[\hat{\rho}_{\text{SE}}(0)] = \hat{\rho}_E(0), \quad (53)$$

$$\hat{\rho}_\alpha = \frac{\text{Tr}_S[(\hat{I}_2 + \hat{\sigma}_\alpha) \otimes \hat{I}_E] \hat{\rho}_{\text{SE}}(0)}{w_\alpha}, \quad (54)$$

with $w_0 = 1$ and $w_\alpha = \text{Tr}[(\hat{I}_2 + \hat{\sigma}_\alpha) \otimes \hat{I}_E] \hat{\rho}_{\text{SE}}(0)$ for $\alpha = x, y, z$. We exploit these generic expressions below.

B. Initial polarization-frequency correlation and B+ decomposition for single photons

We consider initial polarization-frequency correlations by following the recent results and experimental work on generating, in principle, arbitrary single-photon dephasing dynamics [22]. The generic initial polarization-frequency state can be written as

$$|\psi(0)\rangle_{\text{SE}} = C_v |v\rangle \otimes \int d\omega g(\omega) |\omega\rangle + C_h |h\rangle \otimes \int d\omega g(\omega) e^{i\theta(\omega)} |\omega\rangle, \quad (55)$$

where $|C_h|^2 + |C_v|^2 = 1$ and $\int d\omega |g(\omega)|^2 = 1$. Above, the crucial ingredient is the frequency-dependent initial phase $\theta(\omega)$ for the component including the polarization h . If $\theta(\omega)$ is a constant function, then there are no initial system-environment correlations. However, controlling the nonconstant functional form of $\theta(\omega)$ allows control of the initial correlations and their amount.

When the initial state evolves according to the interaction Hamiltonian, Eq. (3), the reduced polarization state at time t is

$$\hat{\rho}(t) = \begin{pmatrix} |C_h|^2 & \kappa(t) C_h C_v^* \\ \kappa(t)^* C_h^* C_v & |C_v|^2 \end{pmatrix}, \quad (56)$$

where the decoherence function is

$$\kappa(t) = \int d\omega |g(\omega)|^2 e^{i\theta(\omega)} e^{-i\Delta n \omega t}. \quad (57)$$

Note that in addition to the frequency probability distribution $|g(\omega)|^2$, one can now use also $\theta(\omega)$, and subsequent initial correlations, to control the dephasing dynamics.

The dynamics given by Eqs. (56) and (57) can be equivalently formulated by using the B+ decomposition. Considering the initial total state in Eq. (55) and applying the B+ decomposition along Eq. (50) and Eqs. (53) and (54), we obtain the environmental terms

$$\hat{\rho}_0 = \int d\omega \int d\omega' g(\omega) g(\omega')^* (|C_h|^2 e^{i[\theta(\omega) - \theta(\omega')]} + |C_v|^2) |\omega\rangle \langle \omega'|, \quad (58)$$

$$\hat{\rho}_x = \frac{1}{w_x} \int d\omega \int d\omega' g(\omega) g(\omega')^* (|C_h|^2 e^{i[\theta(\omega) - \theta(\omega')]} + |C_v|^2 + C_h C_v^* e^{i\theta(\omega')} + C_v C_h^* e^{-i\theta(\omega)}) |\omega\rangle \langle \omega'|, \quad (59)$$

$$\hat{\rho}_y = \frac{1}{w_y} \int d\omega \int d\omega' g(\omega) g(\omega')^* (|C_h|^2 e^{i[\theta(\omega) - \theta(\omega')]} + |C_v|^2 + i C_h C_v^* e^{i\theta(\omega')} - i C_v C_h^* e^{-i\theta(\omega)}) |\omega\rangle \langle \omega'|, \quad (60)$$

$$\hat{\rho}_z = \int d\omega \int d\omega' g(\omega) g(\omega')^* |\omega\rangle \langle \omega'|, \quad (61)$$

with weights

$$w_x = 1 + 2 \int d\omega |g(\omega)|^2 \text{Re}[C_v C_h^* e^{-i\theta(\omega)}], \quad (62)$$

$$w_y = 1 + 2 \int d\omega |g(\omega)|^2 \text{Im}[C_v C_h^* e^{-i\theta(\omega)}], \quad (63)$$

$$w_z = 2|C_h|^2. \quad (64)$$

Each specific term of the B+ decomposition is related to a frequency state ($\hat{\rho}_\alpha$) above and acts on its own input system operator \hat{Q}_α [see Eqs. (51) and (52)]. In the current case, we can combine the contributions of $\hat{\rho}_0$ and $\hat{\rho}_z$ to simplify the decomposition into only three terms. Subsequently, the polarization density matrix at time t is given by

$$\hat{\rho}(t) = \frac{1}{2} \begin{pmatrix} w_z & \kappa_0(t)(i-1) \\ \kappa_0(t)^*(-i-1) & 2-w_z \end{pmatrix} + \frac{1}{2} w_x \begin{pmatrix} 0 & \kappa_x(t) \\ \kappa_x(t)^* & 0 \end{pmatrix} + \frac{1}{2} w_y \begin{pmatrix} 0 & -i\kappa_y(t) \\ i\kappa_y(t)^* & 0 \end{pmatrix}, \quad (65)$$

where the three different decoherence functions are given by

$$\kappa_0(t) = \int d\omega |g(\omega)|^2 e^{-i\Delta n \omega t}, \quad (66)$$

$$\kappa_x(t) = \frac{\int d\omega |g(\omega)|^2 (1 + 2\text{Re}[C_v C_h^* e^{-i\theta(\omega)}]) e^{-i\Delta n \omega t}}{w_x}, \quad (67)$$

$$\kappa_y(t) = \frac{\int d\omega |g(\omega)|^2 (1 + 2\text{Im}[C_v C_h^* e^{-i\theta(\omega)}]) e^{-i\Delta n \omega t}}{w_y}. \quad (68)$$

It is interesting to note here that the decoherence function κ_0 is independent of $\theta(\omega)$ and actually corresponds directly to the case where there are no initial polarization-frequency correlations. The other two functions, κ_x and κ_y , depend also on $\theta(\omega)$ and describe in detail how the initial correlations change the dephasing dynamics.

It is also interesting to compare Eq. (65) with the B+ decomposition for generic dephasing dynamics of a qubit

coupled to a bosonic bath, when qubit and bath are initially correlated [21]. The total Hamiltonian of the qubit and the bosonic bath reads

$$\hat{H} = \omega_q \hat{\sigma}_z + \sum_i \omega_i \hat{b}_i^\dagger \hat{b}_i + \hat{\sigma}_z \otimes \sum_i g_i (\hat{b}_i^\dagger + \hat{b}_i), \quad (69)$$

where ω_q is the qubit's energy level separation (in the $|0\rangle$, $|1\rangle$ basis), \hat{b}_i^\dagger and \hat{b}_i are the bath mode creation and annihilation operators, respectively, and g_i is the coupling strength. Employing the B+ decomposition, the dynamics of the off-diagonal element of the qubit's density matrix in the interaction picture reads [21]

$$\langle 0 | \rho_S(t) | 1 \rangle = \sum_\alpha w_\alpha \langle 0 | \hat{Q}_\alpha | 1 \rangle \chi_{\hat{\rho}_\alpha}(\vec{\xi}_t), \quad (70)$$

where $\chi_{\hat{\rho}_\alpha}(\vec{\xi}_t) = \text{Tr}_B[\hat{\rho}_\alpha \hat{D}(\vec{\xi}_t)]$ is the Wigner characteristic function of the bath state $\hat{\rho}_\alpha$ and $\vec{\xi}_t = (\xi_1(t), \xi_2(t), \dots)$ with

$$\xi_j(t) = 2g_j \left(\frac{1 - e^{i\omega_j t}}{\omega_j} \right).$$

$\hat{D}(\vec{\xi}_t) = \exp(\sum_i \xi_i \hat{b}_i^\dagger + \xi_i^* \hat{b}_i)$ is the Glauber displacement operator. Comparison between Eqs. (65) and (70) reveals that the decoherence functions in our photonic model—corresponding to integral transformations of the frequency probability distribution and frequency-dependent phase $\theta(\omega)$ —play the exact same role as the characteristic functions in the dephasing dynamics of a qubit coupled to a bosonic bath.

Let us go back to the photonic model and see in detail, for some examples, what is the relation between the original decoherence function, (57), and those appearing in the B+ decomposition in Eqs. (66)–(68). In particular, we consider cases similar to those used in [22] to demonstrate arbitrary control of dephasing dynamics. These include a nonpositive (NP) map and Markovian, non-Markovian, and coherence trapping dynamics. In all of the cases below, the frequency distributions used and the values for $\theta(\omega)$ are similar to those considered in Ref. [22], respectively.

Figure 3 shows the magnitude of various decoherence functions for the case of an NP map, i.e., $\kappa(t) > \kappa(0)$. It is easy to check that the off-diagonal term of the density matrix is obtained from $\rho_{hv}(t) = [\kappa_0(t)(i-1) + w_x \kappa_x(t) - i w_y \kappa_y(t)]/2$ and, equivalently, from $\rho_{hv}(t) = \kappa(t) C_h C_v^*$. Thereby, it is evident that if $\kappa_0(t) = \kappa_x(t) = \kappa_y(t) = 0$, for some $t > 0$, then $\kappa(t) = 0$. However, the reverse statement does not always hold. Instead, one can show that whenever $w_x = w_y = 1$, then having identical decoherence functions, $\kappa_0(t) = \kappa_x(t) = \kappa_y(t)$, is sufficient to have zero coherence, i.e., $\kappa(t) = 0$. This is an interesting result making a link between properties of the CP maps obtained in B+ decomposition and the original NP map. In fact, the case discussed in Fig. 3 demonstrates this situation. This is even more evident when considering the real and imaginary parts of the decoherence functions explicitly (see Fig. 4). One can see that the three decoherence functions κ_0 , κ_x , and κ_y are identical when the interaction time is short. Therefore, since we also have $w_x = w_y = 1$, the decoherence function $\kappa(t)$ has zero value in this regime.

The non-Markovian, Markovian, and coherence trapping cases are plotted, respectively, in Figs. 5–7. Looking at

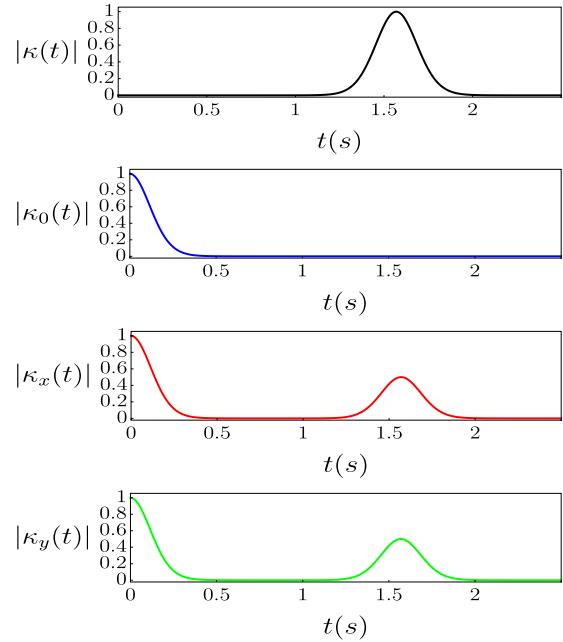


FIG. 3. Nonpositive map decoherence functions. Magnitudes of the original decoherence function (κ) and B+ decomposition decoherence functions (κ_0 , κ_x , κ_y) as a function of time. We set $C_h = C_v = 1/\sqrt{2}$.

Fig. 5, one finds that $|\kappa(t)|$ first decays to 0 and then revives again. This situation displays non-Markovian features, where coherence can revive after a period of disappearance. The Markovian case, however, illustrates a monotonically decaying $|\kappa(t)|$ (see Fig. 6). Finally, in the coherence trapping case we observe that $|\kappa(t)|$ decays at first but mostly maintains its value later (Fig. 7). The magnitudes of the other three decoherence functions, used in the B+ decomposition, are also plotted in the corresponding figures. We observe that these decoherence functions behave similarly, in contrast to the case of an NP map. Again, whenever κ_0 , κ_x , and κ_y are all 0, one has $\kappa(t) = 0$. However, since w_x and w_y are not equal,

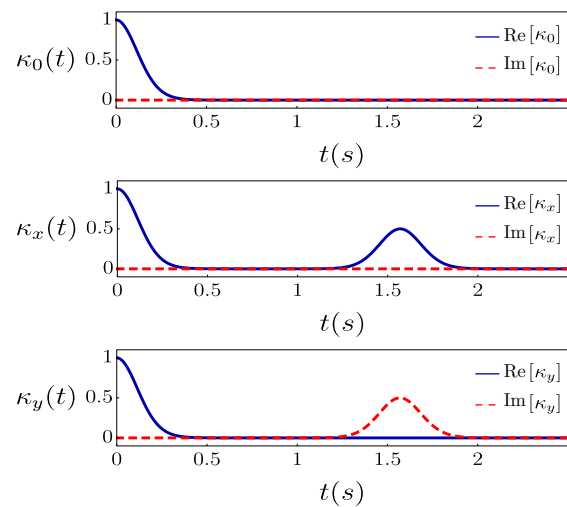


FIG. 4. Nonpositive map decoherence functions. Real and imaginary parts of the B+ decomposition decoherence functions (κ_0 , κ_x , κ_y) as a function of time. We set $C_h = C_v = 1/\sqrt{2}$.

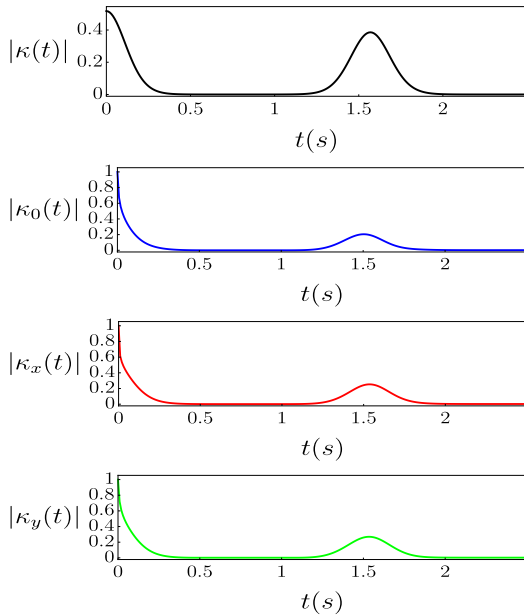


FIG. 5. Non-Markovian dynamics. Magnitudes of the original decoherence function (κ) and B+ decomposition decoherence functions (κ_0 , κ_x , κ_y) as a function of time. We set $C_h = C_v = 1/\sqrt{2}$.

we get a nonzero κ , even though κ_0 , κ_x , and κ_y seem to be identical in some regions.

V. DISCUSSION

We have studied the influence of initial correlations on open-system dynamics from two perspectives corresponding to master equation descriptions and the recently introduced B+ decomposition method. By using a common two-photon dephasing scenario with local polarization-frequency inter-

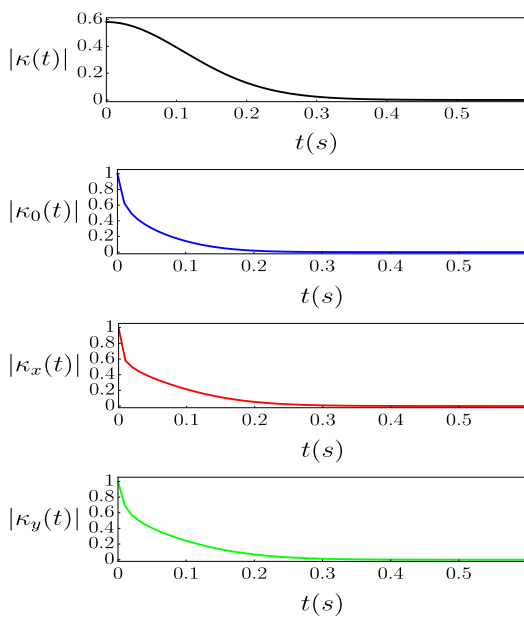


FIG. 6. Markovian dynamics. Magnitudes of the original decoherence function (κ) and B+ decomposition decoherence functions (κ_0 , κ_x , κ_y) as a function of time. We set $C_h = C_v = 1/\sqrt{2}$.

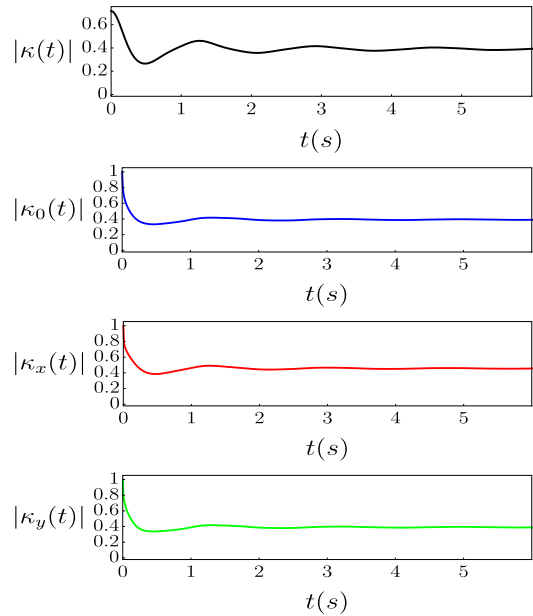


FIG. 7. Coherence trapping dynamics. Magnitudes of the original decoherence function (κ) and B+ decomposition decoherence functions (κ_0 , κ_x , κ_y) as a function of time. We set $C_h = C_v = 1/\sqrt{2}$.

action, our results show explicitly how initial correlations—between the composite environments (frequencies)—influence the decoherence rates and operator form of the master equation for the polarization state. When the environment has a single-peak Gaussian structure, the master equation contains two sets of jump operators, corresponding to the sum and difference between the local interactions, and whose weights can be controlled by changing the amount of initial environmental correlations. Here, the dephasing rates are nonnegative and depend linearly on time for the considered case. With a double-peak bivariate structure, the situation changes drastically. This opens an additional dephasing path with a nonlocal form for the corresponding operator, and the associated rate also has divergences. Moreover, the rates for the other two dephasing operators have distinctive functional forms.

The B+ decomposition method, in turn, allows the study of such cases where the system and environment are initially correlated, preventing the use of conventional CP maps. We have used this decomposition to study dephasing, when the polarization and frequency of a single photon are initially correlated. The results display in detail how the initial correlations change the dephasing contribution arising solely on the initial factorized state. Indeed, instead of having one decoherence function associated with dephasing, we now have three different decoherence functions corresponding to the elements of the B+ decomposition. Here, one of the functions arises due to the initially factorized part and two additional decoherence functions include also contributions from initial polarization-frequency correlations. In general, our results shed light on and help us to understand how different types of correlations influence the dephasing dynamics within the commonly used photonic framework.

ACKNOWLEDGMENTS

S.H.R. acknowledges financial support from the Finnish Cultural Foundation. A.S. acknowledges the support of the EU through the Erasmus+ program and support of the Science and Engineering Research Board, Government of India, through EMR Grant No. EMR/2016/007221.

APPENDIX

General expressions for the elements of the nonzero subspace of the decay rate matrix, denoted $R(t)$, are

$$R_{11}(t) = -\text{Re}[\mathbf{k}_b(t)], \quad (\text{A1})$$

$$R_{12}(t) = \frac{1}{\sqrt{3}}(i\text{Im}[\mathbf{k}_b(t)] - i\text{Im}[\mathbf{k}_a(t)] + i\text{Im}[\Gamma_{ab}(t)] + \text{Re}[\Gamma_{ab}(t)] - \text{Re}[\mathbf{k}_a(t)]), \quad (\text{A2})$$

$$R_{13}(t) = \frac{1}{2\sqrt{6}}(4i\text{Im}[\mathbf{k}_a(t)] + 2i\text{Im}[\mathbf{k}_b(t)] - 3i\text{Im}[\mathbf{k}_{ab}(t)] - i\text{Im}[\Gamma_{ab}(t)] + 4\text{Re}[\mathbf{k}_a(t)] - 3\text{Re}[\mathbf{k}_{ab}(t)] - \text{Re}[\Gamma_{ab}(t)]), \quad (\text{A3})$$

$$R_{21}(t) = R_{12}(t)^*, \quad (\text{A4})$$

$$R_{22}(t) = \frac{1}{3}(-2\text{Re}[\mathbf{k}_a(t)] + \text{Re}[\mathbf{k}_b(t)] - 2\text{Re}[\Gamma_{ab}(t)]), \quad (\text{A5})$$

$$R_{23}(t) = \frac{1}{6\sqrt{2}}(-3i\text{Im}[\mathbf{k}_{ab}(t)] + 6i\text{Im}[\mathbf{k}_b(t)] + 3i\text{Im}[\Gamma_{ab}(t)] - 4\text{Re}[\mathbf{k}_a(t)] - 3\text{Re}[\mathbf{k}_{ab}(t)] + 8\text{Re}[\mathbf{k}_b(t)] - \text{Re}[\Gamma_{ab}(t)]), \quad (\text{A6})$$

$$R_{31}(t) = R_{13}(t)^*, \quad (\text{A7})$$

$$R_{32}(t) = R_{23}(t)^*, \quad (\text{A8})$$

$$R_{33}(t) = \frac{1}{6}(-2\text{Re}[\mathbf{k}_a(t)] - 3\text{Re}[\mathbf{k}_{ab}(t)] - 2\text{Re}[\mathbf{k}_b(t)] + \text{Re}[\Gamma_{ab}(t)]), \quad (\text{A9})$$

where we have defined $\mathbf{k}_i(t) = \frac{1}{\kappa_i(t)} \frac{d}{dt} \kappa_i(t)$, $\Gamma_{ab}(t) = \frac{1}{\Lambda_{ab}(t)} \frac{d}{dt} \Lambda_{ab}(t)$, and $\mathbf{k}_{ab}(t) = \frac{1}{\kappa_{ab}(t)} \frac{d}{dt} \kappa_{ab}(t)$.

-
- [1] H. P. Breuer and F. Petruccione, *The Theory of Open Quantum Systems* (Oxford University Press, Oxford, UK, 2002).
- [2] S. F. Huelga *et al.*, *Open Quantum Systems: An Introduction* (Springer, Berlin, 2012).
- [3] Á. Rivas, S. F. Huelga, and M. B. Plenio, *Rep. Prog. Phys.* **77**, 094001 (2014).
- [4] H.-P. Breuer, E.-M. Laine, J. Piilo, and B. Vacchini, *Rev. Mod. Phys.* **88**, 021002 (2016).
- [5] L. Li, M. J. Hall, and H. M. Wiseman, *Phys. Rep.* **759**, 1 (2018).
- [6] C.-F. Li, G.-C. Guo, and J. Piilo, *EPL (Europhys. Lett.)* **127**, 50001 (2019).
- [7] C.-F. Li, G.-C. Guo, and J. Piilo, *EPL (Europhys. Lett.)* **128**, 30001 (2019).
- [8] I. de Vega and D. Alonso, *Rev. Mod. Phys.* **89**, 015001 (2017).
- [9] E.-M. Laine, H.-P. Breuer, J. Piilo, C.-F. Li, and G.-C. Guo, *Phys. Rev. Lett.* **108**, 210402 (2012).
- [10] B.-H. Liu, D.-Y. Cao, Y.-F. Huang, C.-F. Li, G.-C. Guo, E.-M. Laine, H.-P. Breuer, and J. Piilo, *Sci. Rep.* **3**, 1781 (2013).
- [11] E.-M. Laine, H.-P. Breuer, and J. Piilo, *Sci. Rep.* **4**, 4620 (2014).
- [12] G.-Y. Xiang, Z.-B. Hou, C.-F. Li, G.-C. Guo, H.-P. Breuer, E.-M. Laine, and J. Piilo, *EPL (Europhys. Lett.)* **107**, 54006 (2014).
- [13] B.-H. Liu, X.-M. Hu, Y.-F. Huang, C.-F. Li, G.-C. Guo, A. Karlsson, E.-M. Laine, S. Maniscalco, C. Macchiavello, and J. Piilo, *EPL (Europhys. Lett.)* **114**, 10005 (2016).
- [14] S. H. Raja, G. Karpat, E.-M. Laine, S. Maniscalco, J. Piilo, C.-F. Li, and G.-C. Guo, *Phys. Rev. A* **96**, 013844 (2017).
- [15] P. Pechukas, *Phys. Rev. Lett.* **73**, 1060 (1994).
- [16] R. Alicki, *Phys. Rev. Lett.* **75**, 3020 (1995).
- [17] P. Pechukas, *Phys. Rev. Lett.* **75**, 3021 (1995).
- [18] T. F. Jordan, A. Shaji, and E. C. G. Sudarshan, *Phys. Rev. A* **70**, 052110 (2004).
- [19] A. Shaji and E. C. G. Sudarshan, *Phys. Lett. A* **341**, 48 (2005).
- [20] L. Joseph and A. Shaji, *Phys. Rev. A* **97**, 032127 (2018).
- [21] G. A. Paz-Silva, M. J. W. Hall, and H. M. Wiseman, *Phys. Rev. A* **100**, 042120 (2019).
- [22] Z.-D. Liu, H. Lyyra, Y.-N. Sun, B.-H. Liu, C.-F. Li, G.-C. Guo, S. Maniscalco, and J. Piilo, *Nat. Commun.* **9**, 1 (2018).
- [23] S. Alipour, A. T. Rezakhani, A. P. Babu, K. Mølmer, M. Möttönen, and T. Ala-Nissila, *arXiv:1903.03861*.
- [24] B.-H. Liu, L. Li, Y.-F. Huang, C.-F. Li, G.-C. Guo, E.-M. Laine, H.-P. Breuer, and J. Piilo, *Nat. Phys.* **7**, 931 (2011).
- [25] V. Gorini, A. Kossakowski, and E. C. G. Sudarshan, *J. Math. Phys.* **17**, 821 (1976).
- [26] G. Lindblad, *Commun. Math. Phys.* **48**, 119 (1976).
- [27] G. Guarnieri, A. Smirne, and B. Vacchini, *Phys. Rev. A* **90**, 022110 (2014).
- [28] A. Smirne, D. Egloff, M. G. Díaz, M. B. Plenio, and S. F. Huelga, *Quantum Sci. Technol.* **4**, 01LT01 (2019).

- [29] R. Alicki and K. Lendi, *Quantum Dynamical Semigroups and Applications* (Springer, Berlin, 2007), Vol. 717.
- [30] Á. Rivas, S. F. Huelga, and M. B. Plenio, *Phys. Rev. Lett.* **105**, 050403 (2010).
- [31] G. M. Palma, K. A. Suominen, and A. K. Ekert, *Proc. R. Soc. Lond. A* **452**, 567 (1996).
- [32] J. H. Reina, L. Quiroga, and N. F. Johnson, *Phys. Rev. A* **65**, 032326 (2002).
- [33] M. A. Cirone, G. De Chiara, G. M. Palma, and A. Recati, *New J. Phys.* **11**, 103055 (2009).
- [34] C. Addis, P. Haikka, S. McEndoo, C. Macchiavello, and S. Maniscalco, *Phys. Rev. A* **87**, 052109 (2013).